Site-selective spectroscopy of Tb^{3+} centers in SrF_2 and CaF_2

K. M. Murdoch,* G. D. Jones, and R. W. G. Syme
Department of Physics and Astronomy, University of Canterbury, Christchurch, New Zealand
(Received 3 March 1997)

Laser-selective excitation techniques have been used to establish sets of energy levels for both the fluoride and hydrogenic varieties of the tetragonal symmetry (C_{4v}) centers and for five multihydrogenic centers observed in SrF_2:Tb^{3+} and CaF_2:Tb^{3+}. Infrared-absorption measurements identified additional energy levels for the principal C_{4v} F^- centers and crystal-field fits are reported for these. Polarization studies of the various spectral lines of the C_{4v} F^- centers were used to determine the symmetry labels of energy levels, up to the $^5D_4$ multiplet. Both electric- and magnetic-dipole contributions to the intensities of absorption and fluorescence lines need to be included to account for the observed polarization behavior. The multihydrogenic ion centers exhibit varied forms of bleaching behavior associated with light-induced hydrogenic ion motion. One center is strikingly unusual as it increases in intensity on irradiation in the region of its $^5D_4$ multiplet transitions. $^5D_4$ multiplet fluorescence lifetimes are closely similar for the H^- and D^- varieties of all the hydrogenic centers, indicating essentially radiative lifetimes. [S0163-1829(97)06827-6]

I. INTRODUCTION

In this paper, we present a laser-selective-excitation (LSE) spectroscopic study of Tb^{3+} in CaF_2 and SrF_2 crystals, both before and after hydrogenation. Previous studies of Tb^{3+} spectra in CaF_2 include an initial 77-K fluorescence study,[1] with the spectra interpreted in terms of a single center comprising Tb^{3+} ions in cubic symmetry sites. This was justified on the grounds that lower-symmetry Tb^{3+} centers would exhibit more electric-dipole-allowed transitions than were observed. Subsequently cubic-symmetry crystal-field energy levels for Tb^{3+} were derived,[2] and found to be in close agreement with those observed. The conclusion was that any charge compensation is too remote to alter significantly the energy levels from the proposed cubic symmetry patterns.

A 77-K fluorescence study[3] of CaF_2:Tb^{3+}, with argon-ion laser and nitrogen-laser nonselective excitation of the $^5D_4$ and $^5D_3$ multiplets, revealed a second, weaker intensity Tb^{3+} center, whose transitions appeared on the long-wavelength side of those of the principal center previously observed.[1] Room-temperature and 125-K fluorescence studies[4] of CaF_2:Tb^{3+}, with excitation of the $^5D_4$ multiplet by the blue lines of an argon-ion laser, identified two main groups (I and II) of emission lines. By comparison with the fluorescence of Tb^{3+} ions observed for other host crystals of known rare-earth site symmetry, these two groups were tentatively assigned to centers of C_{4v} and C_{3v} symmetry.

An electron paramagnetic resonance (EPR) study[5] of CaF_2:Tb^{3+} revealed one tetragonal symmetry center and one trigonal symmetry center. The tetragonal center was ascribed to Tb^{3+} ions having nearest-neighbor interstitial F^- ions. For this center, the separation of the two lowest electronic states was measured as 5.134 ± 0.006 GHz (0.17 cm^{-1}), with a ground-state $g_\parallel$ value of 17.77 ± 0.02.

An EPR study[6] of SrF_2:Tb^{3+} identified two tetragonal symmetry centers. The separation of the two close-lying ground levels of the principal tetragonal center was measured through direct observation of the 14.4 ± 0.2 GHz (0.48 cm^{-1}) microwave transition between them, with a ground-state $g_\parallel$ value of 17.95 ± 0.05.

Previous LSE studies of other trivalent rare-earth ions in CaF_2 have established that rare-earth ions preferentially form tetragonal symmetry (A) centers, with additional trigonal symmetry (B) centers present for rare-earth ions toward the lutecium end of the lathanide series. The tetragonal symmetry centers have a charge-compensating F^- ion in the nearest-neighbor interstitial position located in the $\langle 100\rangle$ direction from the rare-earth ion.

For particular rare-earth ions, the principal trigonal centers can be different in SrF_2 and CaF_2 . The principal trigonal symmetry center observed in CaF_2:Er^{3+} is the trigonal B center,[7] while that observed in SrF_2:Er^{3+} is the trigonal J center, and these are spectroscopically distinct. The J center[8] has a next-nearest-neighbor interstitial F^- ion located in the $\langle 111\rangle$ direction from the Er^{3+}, while a definitive model for the trigonal B center of CaF_2 has not been established.[9] In contrast, the principal trigonal symmetry center observed for Ho^{3+} is the trigonal B center in both CaF_2:Ho^{3+} and SrF_2:Ho^{3+}.[10]

Preliminary laser selective excitation results for Tb^{3+} were reported in an earlier brief account.[11] In this paper experimental LSE spectra are presented in Secs. III and IV, the bleaching behavior of low-symmetry hydrogenic centers is described in Sec. V, and fluorescence lifetimes of Tb^{3+} centers are reported in Sec. VI.

II. EXPERIMENTAL TECHNIQUES

CaF_2 and SrF_2 crystals containing 0.05% molar concentrations of Tb^{3+} were grown by the Bridgman-Stockbarger method. Appropriate amounts of the host alkaline-earth fluoride and TbF_3 were placed in a graphite crucible and lowered through the temperature gradient produced by the heating coil of a 38-kW Arthur D. Little R.F. furnace, at a lowering rate of 7 mm h^{-1} over 18 h. Oriented crystals for polarization

studies were cut from boules aligned by their (111) cleavage planes.

High-pressure hydrogenation of CaF_2:Tb^{3+} and SrF_2:Tb^{3+} crystals was carried out at 15-atm hydrogen pressure in a stainless-steel furnace with the crystal samples heated to 900 °C for 1.25 h while in contact with molten aluminum. The cost of deuterium gas precluded similar high-pressure deuteration treatments. Deuterations of CaF_2:Tb^{3+} and SrF_2:Tb^{3+} crystals involved heating the crystal samples in contact with molten aluminum to 850 °C in a $\frac{2}{3}$-atm pressure of deuterium for up to 55 h.

The term *hydrogenic* is used to denote both the hydrogen and deuterium isotopes, while H^- and D^- specify the respective ions of a particular isotopic species. The relative H^- or D^- ion concentrations present in the hydrogenated and deuterated crystals were determined by (a) measuring the line strength of the respective 1919- and 1384-cm^{-1} second-harmonic absorption transitions of the main T_d symmetry center[12] and (b) scaling these by factors of 23 and 39, respectively, to obtain the corresponding relative line strengths for the H^- and D^- fundamentals. From these, the relative populations of H^- and D^- T_d centers could be estimated. The samples hydrogenated at 15-atm pressure were found to have seven times higher concentration of T_d centers than did the samples deuterated at $\frac{2}{3}$-atm pressure.

10-K infrared-absorption spectra were recorded at 0.1-cm^{-1} resolution with a Digilab FTS40 Fourier transform infrared interferometer equipped with a closed-cycle conduction-type helium cryostat. Zeeman infrared-absorption measurements were made with a 4-T superconducting solenoid built into the can of a helium cryostat. The infrared beam was directed along a tube fixed through the center of this solenoid, and the crystal samples were cooled by thermal contact with a copper sample holder screw-fitted into the middle of this tube. With this arrangement, no low-temperature infrared transmitting windows were required.

A Spectra-Physics 375 dye laser pumped by the ultraviolet lines of a Spectra-Physics 2045 argon-ion laser was used for laser excitation of Tb^{3+}. Coumarin 480 dye was appropriate for laser excitation of the electronic transitions to the $^5D_4$ multiplet of Tb^{3+}, with the laser power being typically 5–10 mW. A birefringent tuning element in the dye laser gave a spectral linewidth of 1 cm^{-1}, and allowed continuous tuning of the laser through the fluorescence range of the dye.

The excitation spectra for identifying new Tb^{3+} centers were obtained by scanning the dye laser over the appropriate absorption region of the $^5D_4$ multiplet and monitoring fluorescence from all the centers present with a 3-nm resolution 0.25-m Bausch and Lomb monochromator equipped with a thermoelectrically cooled EMI 9558 photomultiplier. For most of the measurements the monochromator was set to 545 nm, appropriate for detecting $^5D_4 \rightarrow {}^7F_5$ fluorescence transitions. Additional Corning 2-64 filters were included to improve rejection of scattered pump laser radiation from the excitation spectra.

A Spex 1403 double monochromator equipped with a thermoelectrically cooled RCA 31034A photomultiplier recorded the site-selective excitation and fluorescence spectra under computer control. Photon-counting techniques were used to give the high sensitivity needed to detect weak fluorescence lines.

All laser-excited spectra were recorded with crystals mounted on the cold finger of a Cryosystems LTS22.1 closed-cycle cryostat. The sample temperature could be varied from 10 to 300 K, with most spectra recorded at 10 K.

As polarization studies of laser-excited fluorescence spectra can conclusively identify the rare-earth ion site symmetries,[13,14] polarization spectra were recorded using a Spectra-Physics model 310 polarization rotator to vary the laser polarization direction and a polarizer sheet as a fluorescence analyzer. A polarization scrambler equalized the spectrometer response for the different linear polarizations.

10-K $^5D_4$ multiplet fluorescence lifetimes of Tb^{3+} centers were measured using a Photochemical Research Associates (PRA) LN107 dye laser system pumped by a PRA LN1000 pulsed nitrogen laser. The dye laser output comprised 500-ps pulses of 0.04-nm spectral bandwidth and 100-μJ average energy. Coumarin 481 dye was appropriate for the excitation of the $^5D_4$ multiplet. The fluorescence decays were recorded by a Spex 1700 monochromator equipped with a thermoelectrically cooled EMI 9558 photomultiplier tube. A Hitachi model VC6275 digital storage oscilloscope averaged each fluorescent transient for 256 shots. The integrated transients were least-squares fitted to single exponential decays on a constant background for the fluorescence decay times.

III. SPECTROSCOPY OF Tb^{3+} BEFORE HYDROGENATION

A. Energy levels of Tb^{3+} centers

The $4f^8$ configuration, appropriate for Tb^{3+}, has the $^5D_4$ multiplet in the 20 000-cm^{-1} region. A notation of a letter plus a numerical subscript is adopted for labeling the crystal-field levels of various $^{2S+1}L_J$ multiplets. The ground multiplet $^7F_6$ is labeled Z, with the ground state being Z_1, and the first excited multiplet $^7F_5$ labeled by Y. Higher-energy multiplets include the $^7F_4$ through $^7F_0$ set labeled by X through T. The levels of the $^5D_4$ multiplet are labeled $A_1, A_2 \ldots$ in order of increasing energy.

For particular centers, the Tb^{3+} levels have wave functions transforming as one of the irreps of the appropriate point-symmetry group. For centers having Tb^{3+} ions in sites of C_{4v} symmetry, the energy levels transform as one of the five irreps γ_1 to γ_5 of the C_{4v} point group, where the irreps γ_1 to γ_4 are all of single dimension, while γ_5 is of double dimension.

The relative polarization intensities of electric- and magnetic-dipole allowed fluorescence transitions for various electric-dipole-allowed excitation transitions of C_{4v} symmetry centers in the $\langle 100 \rangle$-polarization geometry are reproduced[13] in Table I. These intensities assume equal populations of the three possible orientations of such centers in alkaline-earth fluoride crystals. In the polarization tables the various polarization geometries are specified by $x(ab)z$, in which x defines the direction of propagation of the incident laser beam, z is the direction of propagation of the analyzed fluorescence, $a(y$ or $z)$ defines the polarization (electric vector) of the incident laser light, and $b(x$ or $y)$ defines the polarization of the fluorescence. π-polarized radiation has the E vector along the fourfold symmetry axis of the C_{4v} center and σ-polarized light has its E vector perpendicular to this symmetry axis.

TABLE I. Relative polarization intensities for tetragonal (C_{4v}) centers in ⟨100⟩-oriented crystals. $\gamma_a=\gamma_1,\ \gamma_2,\ \gamma_3,\ \gamma_4$, or γ_5. $\gamma_A=\gamma_1,\ \gamma_2,\ \gamma_3$, or γ_4. The **E**-vector polarizations of the electric-dipole transitions are identified as either π or σ, while those of the magnetic-dipole transitions are either ($\acute{\pi}$) or ($\acute{\sigma}$).

Pump transition Electric dipole	Fluorescence transition Electric dipole	Polarization geometry $x(yy)z$	$x(yx)z$
$\gamma_a\rightarrow\gamma_a(\pi)$	$\gamma_a\rightarrow\gamma_a(\pi)$	1	0
	$\gamma_A\leftrightarrow\gamma_5(\sigma)$	0	1
$\gamma_A\rightarrow\gamma_5(\sigma)$	$\gamma_a\rightarrow\gamma_a(\pi)$	0	1
	$\gamma_A\leftrightarrow\gamma_5(\sigma)$	2	1
Electric dipole	Magnetic dipole		
$\gamma_a\rightarrow\gamma_a(\pi)$	$\gamma_1\leftrightarrow\gamma_2(\acute{\pi})$	0	1
	$\gamma_3\leftrightarrow\gamma_4(\acute{\pi})$	0	1
	$\gamma_5\rightarrow\gamma_5(\acute{\pi})$	0	1
	$\gamma_a\leftrightarrow\gamma_5(\acute{\sigma})$	1	0
$\gamma_A\rightarrow\gamma_5(\sigma)$	$\gamma_1\leftrightarrow\gamma_2(\acute{\pi})$	1	0
	$\gamma_3\leftrightarrow\gamma_4(\acute{\pi})$	1	0
	$\gamma_5\rightarrow\gamma_5(\acute{\pi})$	1	0
	$\gamma_a\leftrightarrow\gamma_5(\acute{\sigma})$	1	2

B. Laser selective excitation and fluorescence spectra

Absorption spectroscopy is the most direct way of determining rare-earth energy levels. However, for Tb^{3+}, the absorption transitions to energy levels of the $^5D_4$ and $^5D_3$ multiplets are sufficiently weak to require crystals of at least 30-mm thickness to record satisfactory absorption spectra of the principal centers and minority hydrogenic centers may remain undetected. In contrast, laser excitation gives enhanced sensitivity spectra, and is preferred for observing the very weak absorption lines of dilute fluorescing centers. Such excitation spectra are obtained when the laser frequency is continuously scanned while selectively monitoring the fluorescence. Either a spectrometer is tuned to a particular transition, specifically to record the excitation spectrum of the corresponding single center, or broadband wavelength selection is used to detect all fluorescing centers present.

Only the $^7F_6\rightarrow{}^5D_4$ absorption transitions of Tb^{3+} lie within the tuning range of coumarin 480 dye, and the laser excited fluorescence spectra were obtained by pumping these transitions. Visible green fluorescence was observed when exciting the strongest $^7F_6\rightarrow{}^5D_4$ transitions and is from the $^5D_4\rightarrow{}^7F_5$ transitions which dominate the fluorescence spectra of all centers, as observed for other Tb^{3+} systems.[15,16] The $^5D_4\rightarrow{}^7F_5$ fluorescence transitions are magnetic dipole allowed with $\Delta J=1$, giving them a significant magnetic-dipole character and strong chiro-optical activity. This is a reason why Tb^{3+} emission has been applied extensively as a probe of lanthanide-ion coordination behavior in solutions and chiral systems.[16] $^5D_4$ multiplet excitation spectra for all Tb^{3+} centers present were obtained by scanning the laser, while monitoring the fluorescence over a 30-nm wavelength range centered around the $^5D_4\rightarrow{}^7F_5$ fluorescence maximum of 545 nm.

In the SrF_2:Tb^{3+} excitation spectrum, the lines of the tetragonal symmetry C_{4v} F^- center dominate [Fig. 1(a)]. This

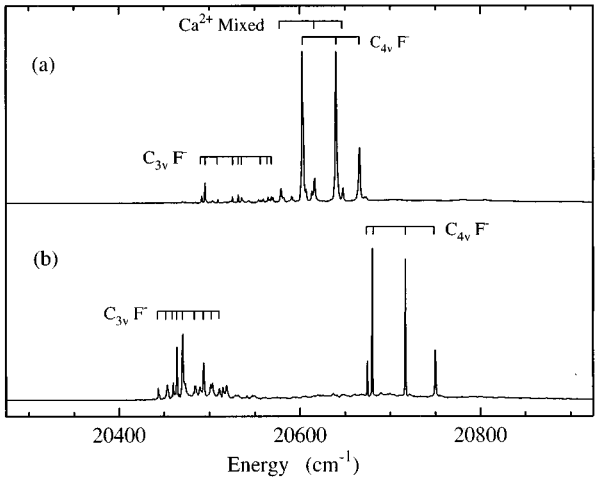

FIG. 1. 10-K excitation spectra of the $^5D_4$ multiplet for (a) SrF_2:0.05%Tb^{3+} and (b) CaF_2:0.05%Tb^{3+}, recorded while monitoring the fluorescence of all Tb^{3+} centers at 545 nm.

center has been identified for many other rare-earth ions in CaF_2 and SrF_2, including Er^{3+}, Ho^{3+}, Pr^{3+}, and Nd^{3+}.[7,10,13,17]

Of other centers present, the two strongest minority centers have excitation lines of comparable intensity. One is the trigonal C_{3v} F^- center, whose Ho^{3+} analog had been reported as the trigonal *B* center[10] in SrF_2:Ho^{3+}. The two principal $^5D_4$ multiplet excitation transitions reported[11] for this C_{3v} F^- center are more than 100 cm^{-1} lower in energy than any of those of the principal C_{4v} F^- center. The other minority center is spectroscopically similar to the main C_{4v} F^- center, with its three reported[11] energy levels all about 20 cm^{-1} lower in energy than the corresponding energy levels of the main C_{4v} F^- center. It is believed to be an on-axis Ca^{2+} modification of the C_{4v} center produced by traces of CaF_2 in the SrF_2 starting material from which the SrF_2:Tb^{3+} crystal was grown. Comparable excitation transitions of mixed Pr^{3+} centers have been reported[14] as satellites to transitions of the parent C_{4v} F^- center. Such an on-axis $Ca^{2+}Tb^{3+}$ center may well account for the second tetragonal center detected by EPR.[6] The corresponding CaF_2:Tb^{3+} excitation spectrum shows two principal centers present at comparable strengths [Fig. 1(b)]. These are the tetragonal (C_{4v}) symmetry *A* center and the trigonal (C_{3v}) symmetry *B* center.

C. Site-selective excitation and fluorescence spectra of Tb^{3+} centers

Site-selective excitation spectra were obtained by monitoring specific $^5D_4\rightarrow{}^7F_5$ fluorescence transitions of each center (Fig. 2). The excitation spectra of all these centers have additional broad vibronic bands higher in energy than the sharp electronic transitions. Such vibronic sidebands have been analyzed for Pr^{3+} C_{4v} centers,[13] and arise from host-lattice phonons coupling to rare-earth electronic states. As the bands observed here for Tb^{3+} do not have a well-defined lattice phonon structure, they were not analyzed in detail.

LSE fluorescence studies were carried out for several specific Tb^{3+} centers, principally for the C_{4v} F^- center, present

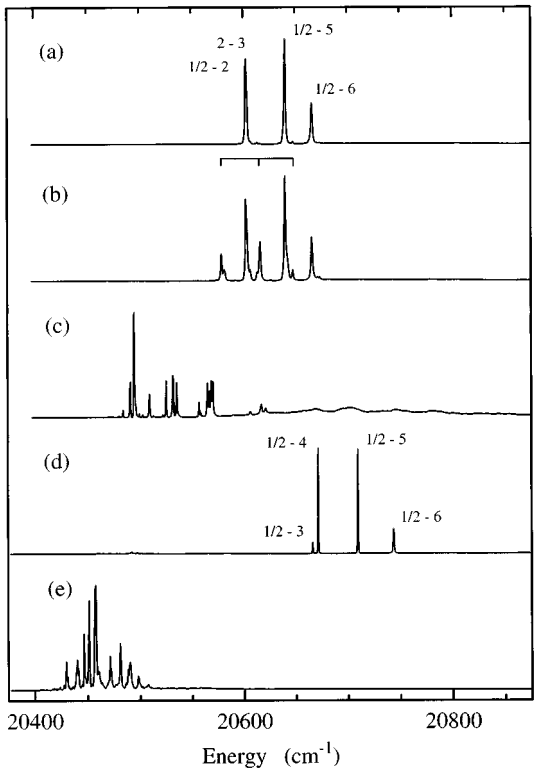

FIG. 2. 10-K excitation spectra of the $^5D_4$ multiplet for (a) the C_{4v} F^- center of SrF_2:0.05%Tb^{3+} (monitoring $A_2 \rightarrow Y_1$ at 18 494 cm^{-1}), (b) the minor C_{4v} F^- mixed center of SrF_2:0.05%Tb^{3+} (monitoring at 18 490 cm^{-1}), (c) the C_{3v} F^- center of SrF_2:0.05%Tb^{3+} (monitoring at 18 459 cm^{-1}), (d) the C_{4v} F^- center of CaF_2:0.05%Tb^{3+} (monitoring $A_1 \rightarrow Y_1$ at 18 468 cm^{-1}), and (e) the C_{3v} F^- center of CaF_2:0.05%Tb^{3+} (monitoring at 18 459 cm^{-1}). Excitation transitions in (a) and (d) are identified by their specific originating $^7F_6$ and terminating $^5D_4$ levels, with 1/2 used for the overlapping A_1 and A_2 levels. The mixed center transitions are indicated in (b).

in both CaF_2:Tb^{3+} and SrF_2:Tb^{3+}. Fluorescence spectra of the $^5D_4 \rightarrow {}^7F_J$ transitions were obtained by selective excitation of the $^5D_4$ multiplet. The similarity of the fluorescence spectrum of the minor tetragonal symmetry center of SrF_2:Tb^{3+} to that of the principal C_{4v} F^- center supports its attribution to a CaF_2 in SrF_2 mixed center.

D. C_{4v} F^- centers in SrF_2 and CaF_2

1. Site-selective fluorescence spectra

10-K laser-selective excitation of the $^5D_4$ multiplet in both CaF_2 and SrF_2 produces fluorescence lines (Figs. 3 and 4), which are assigned as $^5D_4 \rightarrow {}^7F_J$ transitions to the various ^7F_J multiplets (Table II). The energies of the $^7F_6 \rightarrow {}^5D_4$ excitation transitions for the C_{4v} F^- centers give the $^5D_4$ levels listed in Table II. Sharp fluorescence lines were observed in transitions to the lower levels of the $^7F_6$, $^7F_5$, $^7F_4$, and $^7F_3$ multiplets, whereas broader fluorescence lines were observed in transitions to other levels of these ^7F_J multiplets. When the crystal temperature is raised, many of the fluorescence lines increase in intensity, and additional lines appear. This indicates that there is more than one emitting level for the upper $^5D_4$ multiplet being excited.

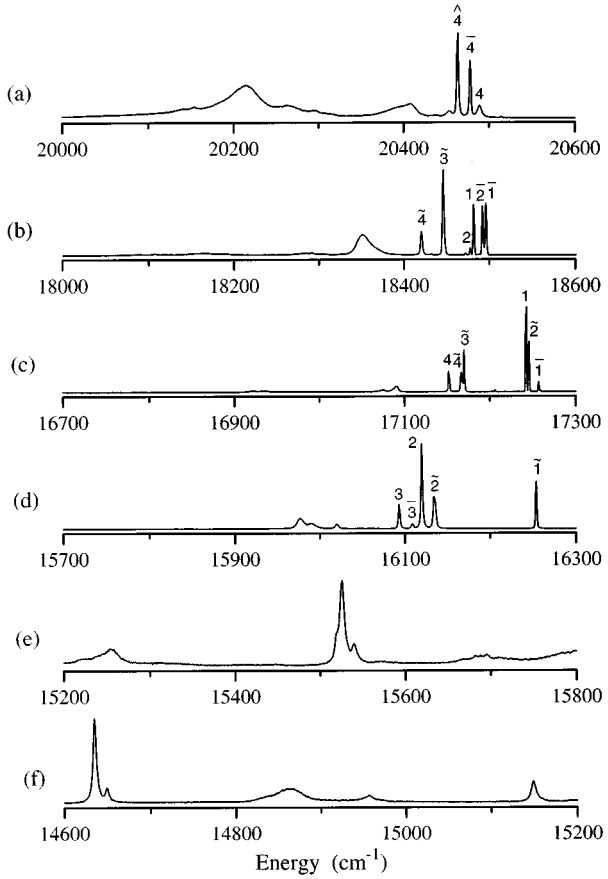

FIG. 3. 10-K fluorescence spectra of the C_{4v} F^- center in the SrF_2:0.05%Tb^{3+} crystal, showing the (a) $^5D_4 \rightarrow {}^7F_6$, (b) $^5D_4 \rightarrow {}^7F_5$, (c) $^5D_4 \rightarrow {}^7F_4$, (d) $^5D_4 \rightarrow {}^7F_3$, (e) $^5D_4 \rightarrow {}^7F_2$, and (f) $^5D_4 \rightarrow {}^7F_1$ and $^7F_0$ transitions. These were recorded while exciting the $Z_1 \rightarrow A_5$ transition at 20 640 cm^{-1}. Terminating levels of transitions are identified by numerical scripts. Originating levels are indicated symbolically by a circumflex for A_4 ($\hat{}$), a tilde for the degenerate levels A_2 and A_3 ($\tilde{}$), a macron for A_2 alone ($\bar{}$), and no symbol for A_1.

2. Infrared-absorption spectra

Infrared spectra show absorption transitions between the ground state and several levels of the $^7F_5$, $^7F_4$, and $^7F_3$ multiplets, and these are included in Table II. The transitions to singlet crystal-field levels identify some γ_3 and γ_4 levels, which are not otherwise observed as they do not terminate fluorescence transitions from the emitting levels of the $^5D_4$ multiplet.

Zeeman infrared spectroscopy was used to distinguish between doublet (γ_5) and singlet levels. Of the observed infrared absorption transitions, the Y_3, X_4, and W_3 upper levels are all assigned as γ_5 levels from their Zeeman splittings. Furthermore, the two almost coincident singlet Z_1 and Z_2 ground levels show a Zeeman splitting through the magnetic moment produced by the Zeeman interaction between them. $g_{(111)}$ values of 9.87 and 10.18 were derived for these ground levels from measured Zeeman splittings of infrared absorption transitions of C_{4v} centers in ⟨111⟩-oriented CaF_2:Tb^{3+} and SrF_2:Tb^{3+}, respectively.

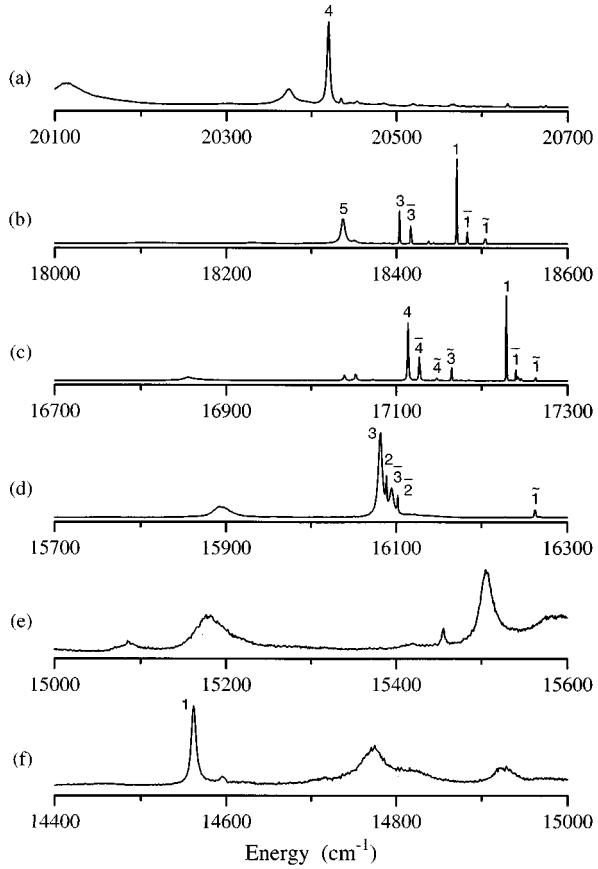

FIG. 4. 10-K fluorescence spectra of the C_{4v} F^- center in the CaF_2:0.05%Tb^{3+} crystal, showing the (a) $^5D_4 \rightarrow {}^7F_6$, (b) $^5D_4 \rightarrow {}^7F_5$, (c) $^5D_4 \rightarrow {}^7F_4$, (d) $^5D_4 \rightarrow {}^7F_3$, (e) $^5D_4 \rightarrow {}^7F_2$, and (f) $^5D_4 \rightarrow {}^7F_1$ and $^7F_0$ transitions. These were recorded while exciting the $Z_1 \rightarrow A_5$ transition at 20 710 cm^{-1}. Terminating levels of transitions are identified by numerical scripts. Originating levels are indicated symbolically by: a circumflex for A_4 ($\hat{}$), a tilde for A_3 ($\tilde{}$), a macron for A_2 ($\bar{}$), and no symbol for A_1.

3. Electronic energy levels and their irrep labels

From these fluorescence spectra, together with the supplementary infrared absorption results, 20 and 22 electronic energy levels were identified for the C_{4v} center in SrF_2 and CaF_2, respectively, as listed in Table II. The C_{4v} irrep labels for the Tb^{3+} energy levels were assigned by considering the appropriate transition selection rules. As the EPR results[5,6] indicate, the ground state consists of almost coincident singlet levels, henceforth labeled Z_1 and Z_2. In SrF_2:Tb^{3+}, transitions from either of these ground levels of the $^7F_6$ multiplet to the lowest level A_1 of the $^5D_4$ multiplet are not observed, indicating zero electric- and magnetic-dipole moments for these transitions. Hence, both the upper A_1 and each of the lower Z_1 and Z_2 levels must be singlets. Additionally, because a fluorescence line from the A_1 level of the $^5D_4$ multiplet to the singlet γ_1 level of the ^7F_o multiplet is observed, the A_1 level is necessarily γ_1, and hence the Z_1 and Z_2 ground states are each either γ_3 or γ_4.

In CaF_2:Tb^{3+}, as none of the Z_1, $Z_2 \rightarrow A_1$ and Z_1, $Z_2 \rightarrow A_2$ transitions were observed, both the A_1 and A_2 levels must be either γ_1 or γ_2. From these initial irrep assignments, the irrep labels of other levels were inferred.

TABLE II. Experimental 10-K energy levels for the C_{4v} F^- centers in CaF_2:0.05%Tb^{3+} and SrF_2:0.05%Tb^{3+} crystals. They are for vacuum in units of cm^{-1}, with an uncertainty of ± 0.5 cm^{-1}. The calculated levels were obtained by fitting a parametric Hamiltonian to the experimental levels, which included C_{4v} symmetry crystal-field terms. All the energy levels are labeled by their C_{4v} symmetry irreps.

			CaF_2:Tb^{3+}		SrF_2:Tb^{3+}	
Multiplet	Level	Irrep	Calc.	Obs.	Calc.	Obs.
$^7F_6$	Z_1	γ_3	1.8	0.0	2.2	0.0
	Z_2	γ_4	1.9	0.0	2.6	0.0
	Z_3	γ_5	193.9		125.6	
	Z_4	γ_1	227.6	215.0	134.7	128.7
	Z_5	γ_3	250.8		139.6	
	Z_6	γ_5	292.0		183.3	
	Z_7	γ_2	323.5		221.4	
	Z_8	γ_1	558.7		383.8	
	Z_9	γ_5	569.5		388.6	
	Z_{10}	γ_4	579.7		394.3	
$^7F_5$	Y_1	γ_2	2158.1	2164.2	2103.9	2109.5
	Y_2	γ_1	2158.1		2106.6	2113.2
	Y_3	γ_5	2223.1	2231.3	2151.0	2160.0
	Y_4	γ_3	2291.7	2283.2	2183.6	2185.7
	Y_5	γ_5	2291.2	2298.7	2212.5	
	Y_6	γ_2	2408.2		2284.5	
	Y_7	γ_5	2514.5		2383.6	
	Y_8	γ_4	2595.9		2453.6	
$^7F_4$	X_1	γ_1	3406.6	3407.1	3348.0	3348.8
	X_2	γ_4	3436.6	3429.5	3367.7	3361.6
	X_3	γ_3	3506.8	3505.7	3441.5	3437.8
	X_4	γ_5	3525.2	3522.4	3438.2	3441.2
	X_5	γ_2	3598.2	3597.0	3502.3	
	X_6	γ_5	3767.3		3639.4	
	X_7	γ_1	4016.5		3838.4	
$^7F_3$	W_1	γ_3	4417.2	4407.9	4368.7	4353.4
	W_2	γ_3	4543.3	4548.2	4475.8	4472.2
	W_3	γ_5	4558.9	4555.1	4486.5	4497.1
	W_4	γ_4	4722.8		4480.7	
	W_5	γ_5	4740.6		4591.3	
$^7F_0$	T_1	γ_1	6062.9	6070.5	5939.5	
$^5D_4$	A_1	γ_1	20635.9	20632.4	20590.2	20587.2
	A_2	γ_2	20659.4	20645.7	20591.1	20603.0
	A_3	γ_5	20645.7	20666.0	20587.5	20604.1
	A_4	γ_4	20646.5	20672.0	20613.9	20616.6
	A_5	γ_3	20725.9	20710.3	20656.3	20640.2
	A_6	γ_5	20756.2	20743.5	20678.0	20666.1
	A_7	γ_1	20785.0			

The interpretation of measured polarization ratios obtained from polarized fluorescence spectra can lead to definitive assignments of irrep labels for experimentally determined energy levels. Such assignments have been successfully made for Ho^{3+} and Pr^{3+} C_{4v} centers in CaF_2

TABLE III. Free-ion and crystal-field parameters, in units of cm^{-1}, for the C_{4v} F^- centers in SrF_2:0.05%Tb^{3+} and CaF_2:0.05%Tb^{3+}. Uncertainties in the parameter values are given in parentheses. Parameter values in square brackets were fixed during the fitting.

	CaF_2		SrF_2	
F^2	[90 426]		[90 426]	
F^4	58 572	(35)	58 934	(30)
F^6	[47 252]		[47 252]	
ζ	1686	(9)	1698	(7)
B_C^4	−1330	(30)	−1101	(32)
B_C^6	624	(20)	474	(20)
B_A^2	807	(23)	482	(20)
B_A^4	504	(24)	450	(23)
B_A^6	445	(30)	334	(27)

and SrF_2 .[10,13] However, for the Tb^{3+} C_{4v} F^- centers here, the selective excitation of transitions gave a wide range of polarization ratios, often quite different from the 2:1 and 0:1 ratios or 0:1 and 1:0 ratios predicted for electric-dipole allowed transitions in C_{4v} symmetry.[13] Many of the weaker fluorescence transitions exhibit ratios close to 1:1. Hence it is not possible to assign irrep labels from the experimentally observed polarization ratios on the basis of purely electric-dipole-allowed transitions. To account for the observed ratios, it is necessary to consider the superimposed effects of electric- and magnetic-dipole-allowed transitions, as discussed in Sec. III D 6.

4. Crystal-field analyses

Energy-level fits to the observed Tb^{3+} C_{4v} F^- center levels were performed using the f-shell empirical programs of Reid, together with the reported Tb^{3+} free-ion parameters[18] (Table III). The crystal-field Hamiltonian H_{CF} used, appropriate for C_{4v} symmetry, has the form

$$H_{CF}=B_C^2C_A^{(2)}+B_C^4[C_0^{(4)}+\sqrt{\tfrac{5}{14}}(C_4^{(4)}+C_{-4}^{(4)})]+B_A^4[C_0^{(4)}-\sqrt{\tfrac{7}{10}}(C_4^{(4)}+C_{-4}^{(4)})]+B_C^6[C_0^{(6)}-\sqrt{\tfrac{7}{2}}(C_4^{(6)}+C_{-4}^{(6)})]+B_A^6[C_0^{(6)}+\sqrt{\tfrac{1}{14}}(C_4^{(6)}+C_{-4}^{(6)})].$$

The initial crystal-field parameters for the Tb^{3+} C_{4v} F^- center fit were obtained by interpolation from those reported for Ho^{3+} and Er^{3+}, and gave predicted energy levels within 16 cm^{-1} of those observed. The agreement was sufficiently good to give confidence in the irrep assignments for the various levels, and all these are fully in agreement with the irrep possibilities deduced from the absence or occurrence of particular spectral lines.

Refinements of these crystal-field fits were made by allowing one of the F^k (F^4 was chosen) and the ζ free-ion parameters and all the crystal-field parameters to vary. The parameter fits all converged uniquely to those listed in Table III. These C_{4v} F^- center crystal-field parameters for Tb^{3+} are comparable to those reported for Nd^{3+}, Ho^{3+}, and Er^{3+}. The resulting energy level fits have rms deviations of less than 13 cm^{-1} for 20 and 22 fitted levels for SrF_2 and CaF_2, respectively.

5. Ground-state wave functions

The ground-state energy levels of the Tb^{3+} C_{4v} F^- centers are noteworthy in comprising two orbital singlets γ_3 and γ_4 separated by just 0.17 and 0.48 cm^{-1} for CaF_2 and SrF_2 , respectively. The crystal-field fit of Table II shows these almost degenerate singlet levels. The cubic-crystal-field $J=6$ energy-level diagram[19] is applicable to the ground multiplet of Tb^{3+}. The cubic-crystal-field parameters B_C^4 and B_C^6 of Table III correspond to a fourth to sixth degree ratio X of close to 0.82, for which the $J=6$ diagram has the three lowest energy levels Γ_2, Γ_3, and $\Gamma_5^{(2)}$ coincident in energy. Inclusion of the second-degree crystal-field term $B_A^2C_0^{(2)}$ gives two lowest-lying energy levels $\Gamma_3\gamma_3$ and $\Gamma_5^{(2)}\gamma_4$ with crystal-field wave functions closely approximating

$$\Gamma_3\gamma_3:\frac{1}{\sqrt{2}}(|6\rangle+|-6\rangle) \quad \text{and} \quad \Gamma_5\gamma_4:\frac{1}{\sqrt{2}}(|6\rangle-|-6\rangle).$$

For these wave functions, the second-degree crystal-field energy shifts are the same for each level, at $B_A^2\langle 6|C_0^{(2)}|6\rangle$, thus maintaining their energy coincidence. The parallel Zeeman interaction between these degenerate singlet levels is $9\mu_BB$, yielding an effective $g_\parallel$ value of 18, close to the EPR values.[5,6] The near coincidence of two singlet levels for the ground states of Tb^{3+} in these C_{4v} F^- centers for CaF_2 and SrF_2 accounts for the observed large $g_{\langle 111\rangle}$ values and for the EPR g_{11} values.

6. Analysis of the polarization behavior of transitions for the SrF_2 center

To understand the complicated polarization behavior of spectral transitions of the Tb^{3+} C_{4v} F^- centers, transition-intensity calculations were performed to evaluate both electric- and magnetic-dipole contributions to the transition intensities. The C_{4v} crystal-field wave functions obtained from the crystal-field fits were used, together with A_{tp}^λ intensity parameters, whose values were estimated on a point-charge point-dipole model, in a manner similar to that of related calculations[20] for other lanthanide complexes. The A_{tp}^λ parameters obtained are (in units of 10^{-12})

$$A_{10}^2=720, \quad A_{30}^2=-58, \quad A_{30}^4=48, \quad A_{50}^4=-23,$$

$$A_{54}^4=12, \quad A_{50}^6=260, \quad A_{54}^5=-140,$$

$$A_{70}^6=0.065 \quad \text{and} \quad A_{74}^6=0.15.$$

In the approximation that the lowest γ_3 and γ_4 singlet levels of the $^7F_6$ multiplet (just 0.48 cm^{-1} apart) can be treated as being a single degenerate level, the transition intensity analysis shows four allowed absorption transitions to the $^5D_4$ multiplet, in agreement with the observed excitation spectra presented in Figs. 1(a) and 2(a). All four transitions are both electric and magnetic dipole allowed, with the electric-dipole

TABLE IV. Polarization ratios $x(yx)z$:$x(yy)z$ for specific excitation and fluorescence transitions of the C_{4v} F^- center in the SrF_2:0.05%Tb^{3+} crystal. Since the A_2 and A_3 levels could not be resolved by the monochromator, the polarization ratios of overlapping fluorescence transitions from these levels were determined by adding the contributions from the unresolved transitions, weighted according to their calculated intensities.

Transitions		E dipole		M dipole		Polarization ratios	
Excitation	Fluorescence	%	Ratio	%	Ratio	Predicted	Measured
$Z_1(\gamma_3)\rightarrow A_5(\gamma_3)$	$A_1(\gamma_1)\rightarrow Z_4(\gamma_1)$	100	0:1			0	0.14
	$A_2(\gamma_5)\rightarrow Z_4(\gamma_1)$	99	1:0	1	0:1	99	5.4
$Z_1(\gamma_3),Z_2(\gamma_4)\rightarrow A_6(\gamma_5)$	$A_1(\gamma_1)\rightarrow Z_4(\gamma_1)$	100	1:0			∞	7.9
	$A_2(\gamma_5)\rightarrow Z_4(\gamma_1)$	99	1:2	1	2:1	0.51	0.58
$Z_1(\gamma_3)\rightarrow A_5(\gamma_3)$	$A_1(\gamma_1)\rightarrow Y_1(\gamma_2)$			100	1:0	∞	9.6
	$A_2(\gamma_5)\rightarrow Y_1(\gamma_2)$	54	1:0	46	0:1	1.17	0.48
$Z_1(\gamma_3),Z_2(\gamma_4)\rightarrow A_6(\gamma_5)$	$A_1(\gamma_1)\rightarrow Y_1(\gamma_2)$			100	0:1	0	0.15
	$A_2(\gamma_5)\rightarrow Y_1(\gamma_2)$	54	1:2	46	2:1	0.96	0.90
$Z_1(\gamma_3)\rightarrow A_5(\gamma_3)$	$A_1(\gamma_1)\rightarrow Y_2(\gamma_1)$	100	0:1			0	0.17
	$A_2(\gamma_5)\rightarrow Y_2(\gamma_1)$	61	1:0	39	0:1	1.56	0.44
$Z_1(\gamma_3),Z_2(\gamma_4)\rightarrow A_6(\gamma_5)$	$A_1(\gamma_1)\rightarrow Y_2(\gamma_1)$	100	1:0			∞	7.8
	$A_2(\gamma_5)\rightarrow Y_2(\gamma_1)$	61	1:2	39	2:1	0.86	0.86
$Z_1(\gamma_3)\rightarrow A_5(\gamma_3)$	$A_2(\gamma_5)\rightarrow Y_4(\gamma_3)$	90	1:0	10	0:1	9.0:1	
	$A_3(\gamma_4)\rightarrow Y_4(\gamma_3)$			100	1:0	1:0	
						10.5	3.7
$Z_1(\gamma_3),Z_2(\gamma_4)\rightarrow A_6(\gamma_5)$	$A_2(\gamma_5)\rightarrow Y_4(\gamma_3)$	90	1:2	10	2:1	0.58:1	
	$A_3(\gamma_4)\rightarrow Y_4(\gamma_3)$			100	0:1	0:1	
						0.47	0.61
$Z_1(\gamma_3)\rightarrow A_5(\gamma_3)$	$A_1(\gamma_1)\rightarrow X_1(\gamma_1)$	100	0:1			0	0.14
$Z_1(\gamma_3),Z_2(\gamma_4)\rightarrow A_6(\gamma_5)$		100	0:1			∞	7.5
$Z_1(\gamma_3)\rightarrow A_5(\gamma_3)$	$A_2(\gamma_5)\rightarrow X_3(\gamma_3)$	99	1:0	1	0:1	99:1	
	$A_3(\gamma_4)\rightarrow X_3(\gamma_3)$			100	1:0	1:0	
						99	6.9
$Z_1(\gamma_3),Z_2(\gamma_4)\rightarrow A_6(\gamma_5)$	$A_2(\gamma_5)\rightarrow X_3(\gamma_3)$	99	1:2	1	2:1	0.51:1	
	$A_3(\gamma_4)\rightarrow X_3(\gamma_3)$			100	0:1	0:1	
						0.50	0.45
$Z_1(\gamma_3)\rightarrow A_5(\gamma_3)$	$A_1(\gamma_3)\rightarrow X_4(\gamma_5)$	100	1:0	0	0:1	∞	6.18
$Z_1(\gamma_3),Z_2(\gamma_4)\rightarrow A_6(\gamma_5)$		100	1:2	0	2:1	0.5	0.60
$Z_1(\gamma_3),Z_2(\gamma_4)\rightarrow A_6(\gamma_5)$	$A_2(\gamma_5)\rightarrow W_1(\gamma_3)$	0	1:2	100	2:1	2:1	
	$A_3(\gamma_4)\rightarrow W_1(\gamma_3)$			100	0:1	0:1	
						0.84	1.21

contribution to the total intensity being at least two orders of magnitude larger than the corresponding magnetic-dipole contribution in each case.

Fluorescence transitions from the $^5D_4$ multiplet to other ^7F_J multiplets have significantly more magnetic-dipole character than those to the $^7F_6$ ground multiplet. The most intense fluorescence transitions from the lowest $A_1(\gamma_1)$ level of the $^5D_4$ multiplet to levels of the $^7F_5$, $^7F_4$, and $^7F_3$ multiplets are either purely magnetic-dipole-allowed transitions or have magnetic-dipole intensity contributions comparable to the electric-dipole-allowed intensities. Likewise, transitions originating from γ_5 levels, such as the $A_3(\gamma_5)$ level of the $^5D_4$ multiplet for both SrF_2 and CaF_2, to levels of the $^7F_5$, $^7F_4$, and $^7F_3$ multiplets also exhibit large magnetic-dipole intensity components. In general, the $^5D_4\rightarrow{}^7F_3$, $^7F_4$, and $^7F_5$ fluorescence transitions are of mixed electric- and magnetic-dipole character, whereas fluorescence transitions to the other ^7F_J multiplets are principally electric dipole in character.

From the transition-intensity calculations, the polarization ratios of fluorescence transitions for specific excitation transitions have been predicted, again assuming equal populations of the three possible C_{4v} center orientations. These are compared to the observed ratios measured for the SrF_2 C_{4v} F^- center in Table IV. Where there are unresolved transitions, the contributions from all the transitions must be added to obtain an overall polarization ratio. This is necessary for the unresolved fluorescence transitions from the A_2 and A_3 levels of the $^5D_4$ multiplet for SrF_2. As many of the observed fluorescence transitions have both electric- and

magnetic-dipole contributions, each with quite different polarization ratios, their net polarization ratios differ substantially from the purely electric-dipole ratios.

For the pure electric- or magnetic-dipole-allowed transitions, there is very good agreement between the calculated and observed polarization ratios, and the measured ratios obtained are comparable in quality to those measured for Ho^{3+} and Pr^{3+} C_{4v} centers in SrF_2.[10,13] For the mixed electric- and magnetic-dipole transitions, there is generally good agreement between the calculated and experimental ratios. This agreement is very satisfactory considering that the calculations can provide only relative electric- and magnetic-dipole contributions, and the polarization ratios for the mixed-transition-moment transitions are particularly sensitive to the partitioning.

Although the polarization behavior of the Tb^{3+} C_{4v} centers proved more complicated than the previously studied pure electric-dipole-allowed transition cases of Pr^{3+}, Ho^{3+}, and Er^{3+}, the measured polarization ratios unambiguously assign irreps to the Y_1 and Y_2 energy levels, and confirm the C_{4v} site symmetry of the principal Tb^{3+} C_{4v} center.

IV. SPECTROSCOPY OF Tb^{3+} IN CaF_2 AND SrF_2 AFTER HYDROGENATION

A. Excitation spectra of hydrogenic centers

Excitation spectra of all the Tb^{3+} centers present in the hydrogenated and deuterated crystals were obtained by scanning the laser while monitoring the $^5D_4 \rightarrow {}^7F_5$ fluorescence around 545 nm. Both the heavily hydrogenated CaF_2:Tb^{3+} and SrF_2:Tb^{3+} crystals have markedly different excitation spectra from their parent crystals, Figs. 5(a) and 5(c). The excitation lines of the C_{4v} F^- center barely remain discernible among the many intense new excitation lines produced by the high-pressure hydrogenation treatment. For both CaF_2 and SrF_2, there are two main groups of new excitation lines. One group has lines at energies similar to those of the parent C_{4v} F^- center and may be associated with it. The other group has new lines in the same spectral region as the trigonal C_{3v} F^- center.

The excitation spectrum of the CaF_2:Tb^{3+}:D^- crystal which had been deuterated and then stored for two years was comparable to that of CaF_2:Tb^{3+}:H^-, with the excitation lines of the Tb^{3+} C_{4v} F^- center of minor intensity compared to the new lines produced by deuteration. As for the hydrogenated crystals, two groups of excitation lines occurred, associated with the C_{4v} F^- and C_{3v} F^- centers, Fig. 5(b).

In contrast, the freshly deuterated SrF_2:Tb^{3+} crystal had an excitation spectrum dominated by the excitation lines of the parent C_{4v} F^- center with only weak new lines attributed to D^- modifications of this center, Fig. 5(d). As is to be expected from the very different storage times of the CaF_2 and SrF_2 samples since deuteration, considerably more ambient temperature diffusion of D^- had occurred in the CaF_2 crystal, leading to the formation of more diverse D^- centers for this host.

B. Selective excitation spectra

Site-selective excitation spectra were obtained by monitoring specific $^5D_4 \rightarrow {}^7F_5$ fluorescence transitions of each center. Figure 6 shows the excitation spectra for the CaF_2:Tb^{3+}:D^- crystal. By judicious choice of the transitions being monitored, good selectivity between the different centers was achieved. Only those hydrogenic centers with excitation lines in the same spectral region as those of the parent Tb^{3+} C_{4v} F^- center were studied here in detail. This was because the family of hydrogenic ion centers derived from the C_{4v} F^- center were expected to have spectroscopic and bleaching behavior paralleling that of the hydrogenic Pr^{3+} centers.[21,22]

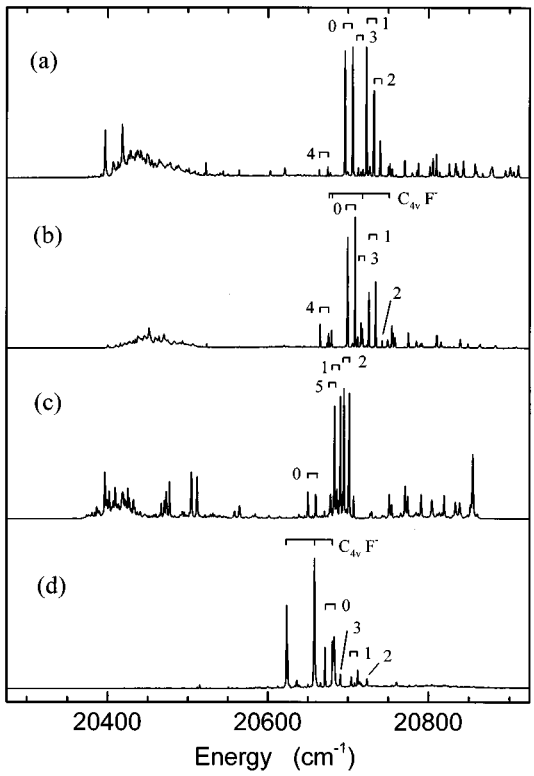

FIG. 5. 10-K excitation spectra of the $^5D_4$ multiplet for (a) hydrogenated CaF_2:0.05%Tb^{3+}, (b) deuterated CaF_2:0.05%Tb^{3+}, (c) hydrogenated SrF_2:0.05%Tb^{3+}, and (d) deuterated SrF_2:0.05%Tb^{3+}. These were recorded while monitoring the fluorescence of all Tb^{3+} centers at 545 nm. Numerical labels identify excitation lines of specific LS centers.

The energies of the $^7F_6 \rightarrow {}^5D_4$ excitation transitions are listed in Table V for each hydrogenic center. Isotope shifts of a few cm^{-1} are observed between the energies of corresponding transitions of hydrogen and deuterium varieties of a given hydrogenic center, and confirm the hydrogenic nature of these centers. Such isotope shifts are exhibited by all hydrogenic rare-earth centers.[23]

The principal new center observed for both deuterated CaF_2 and SrF_2 was expected to be the C_{4v} D^- center, which is derived from the C_{4v} F^- center by the substitution of a D^- ion for the interstitial F^- ion. However, the number of lines and the energy-level patterns differ sufficiently from those of the C_{4v} F^- center to make such an assignment doubtful, and this center is arbitrarily identified as a low-symmetry LS(0) center. The corresponding LS(0) H^- center is less apparent in the spectra of the heavily hydrogenated crystals, as multiple-hydrogenic ion centers have been formed preferentially.

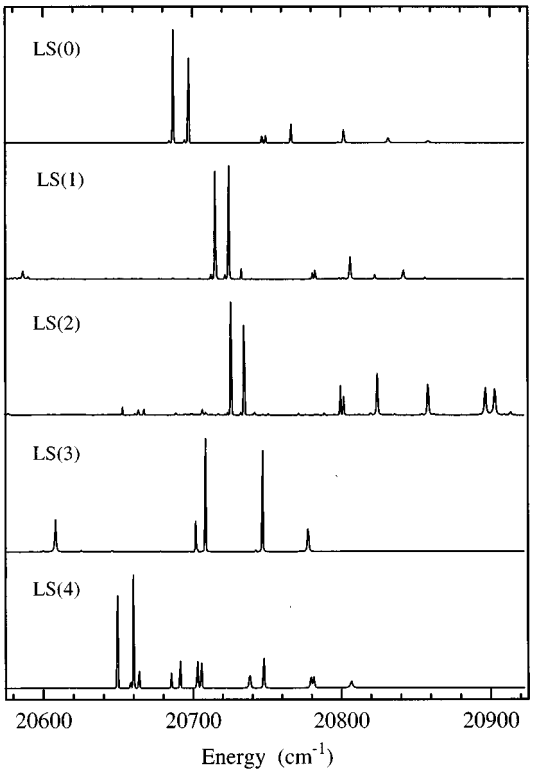

FIG. 6. 10-K selective excitation spectra of the $^5D_4$ multiplet for deuterated CaF_2:0.05%Tb^{3+}, while monitoring the LS(0) center fluorescence at 18 429 cm^{-1}, the LS(1) center at 18 410 cm^{-1}, the LS(2) center at 18 357 cm^{-1}, the LS(3) center at 18 450 cm^{-1}, and the LS(4) center at 18 402 cm^{-1}.

The hydrogenic LS(0) centers for both SrF_2:Tb^{3+} and CaF_2:Tb^{3+} have similar excitation spectra. Each has two strong transitions to the two lowest levels of the $^5D_4$ multiplet, accompanied by five higher-energy transitions, which are an order of magnitude weaker. Transitions to all seven $^5D_4$ multiplet levels are therefore observed, with the third level unexpectedly, but clearly, split into two components. The observation of all seven levels of the $^5D_4$ multiplet in absorption indicates a Tb^{3+} site symmetry lower than C_{4v}, as would be obtained by an off-axis displacement of the charge-compensating hydrogenic ion or the presence of additional substitutional H^- ions adjacent to the Tb^{3+} ions.

Four other hydrogenic centers were observed in both the hydrogenated and deuterated CaF_2 crystals. As these centers are believed to be low-symmetry multihydrogenic ion modifications of the hydrogenic C_{4v} centers, they have been labeled LS(1) through LS(4). The excitation spectra of the LS(0), LS(1), LS(2), and LS(4) centers are similar, with all having two strongest excitation transitions to the two lowest levels of the $^5D_4$ multiplet (Fig. 6). A further center, LS(5), was found only for the heavily hydrogenated crystal, and has markedly different excitation transitions from the other hydrogenic centers.

The excitation spectrum of the LS(3) center differs in having four of its five transitions forming a pattern comparable to that observed for the parent C_{4v} F^- center, but with a more extended $^5D_4$ multiplet pattern than any other Tb^{3+} center. Furthermore, the LS(3) center has fewer excitation and fluorescence transitions than any other Tb^{3+} center. The fact that it also shows polarized bleaching suggests it is a multi-D^--ion C_{4v} symmetry Tb^{3+} center.

Corresponding LS(1), LS(2), LS(3), and LS(5) centers were also observed for the SrF_2 crystals (Fig. 7). They were identified from their comparable excitation and fluorescence spectra, and by the relative energies of their excitation transitions. Again, the LS(5) center was found only for the heavily hydrogenated crystal.

The broadband excitation spectrum of all centers was obtained by monitoring the fluorescence around 535 nm, and indicates the relative populations of the different hydrogenic centers present. During hydrogenation, the H^- or D^- ions are expected to create first hydrogenic C_{4v} centers by their substitution for the interstitial F^- ion of the C_{4v} F^- center, but the LS(0) center which appears strongest is of lower symmetry than C_{4v}. Over time, or by longer hydrogenation treatment, the LS center populations increase in the sequence LS(1), LS(2), and LS(5), with the LS(5) center observed only in crystals with extended hydrogenation treatment. This LS(1), LS(2), LS(5) center ordering parallels that observed for $Pr^{3+}C_S$ centers.[21] The LS(3) and LS(4) centers remain minority centers throughout, with their lines of only low intensity relative to those of the LS(1) and LS(2) centers.

C. Laser-selective-excited fluorescence spectra

Fluorescence spectra comprising the $^5D_4 \rightarrow {}^7F_5$ transitions were obtained by selectively exciting each center in turn (Figs. 8 and 9). Figure 9 shows the fluorescence spectra for CaF_2:Tb^{3+}:H^-. All the fluorescence spectra are similar, with the LS(0) and LS(4) centers bearing particular resemblance to one another. Some of the fluorescence transitions of the LS(1) and LS(2) centers show various splittings, similar to those reported for Pr^{3+} hydrogenic C_S centers,[13] whereas the fluorescence transitions of the LS(0) H^- and LS(0) D^- centers remain unsplit.

V. BLEACHING OF HYDROGENIC LS CENTERS

Multihydrogenic rare-earth centers all exhibit polarized bleaching, with the intensity of their fluorescence observed to decrease on pumping their excitation transitions.[24] Some of these multihydrogenic centers exhibit reversible polarized bleaching with recovery of their original fluorescence intensity on switching the incident laser polarization by 90°. The whole gamut of bleaching behavior has been studied already in detail for the Pr^{3+} C_S centers and models proposed.[21]

A. LS center bleaching

Bleaching was observed for LS(1), LS(2), LS(3), and LS(4), centers and not investigated for the LS(5) center. No bleaching was found for any of the parent hydrogenic C_{4v} centers [the LS(0) centers here], as was the case for the corresponding Pr^{3+}, Nd^{3+}, and Er^{3+} C_{4v} centers.[24] The relative bleaching rates of the H^- and D^- varieties of a given LS center differ, with each H^- center bleaching more rapidly than its equivalent D^- center. For the same incident laser power, the LS(1) H^- center of CaF_2 bleaches seven times faster than the LS(1) D^- center, while the LS(2) H^- center bleaches just 1.3 times faster than the LS(2) D^- center. These differences in bleaching rate are less pronounced than those found for the Pr^{3+} C_S bleachable centers.[21]

TABLE V. Experimental 10-K energy levels of the $^5D_4$ multiplet for hydrogenic centers in CaF_2:0.05%Tb^{3+} and SrF_2:0.05%Tb^{3+} crystals. These are for vacuum in units of cm^{-1}, with an uncertainty of ± 1 cm^{-1}. Values given to one decimal place have a smaller uncertainty of ± 0.2 cm^{-1}. The separations of close levels are given separately.

	CaF_2				SrF_2			
Center	H−		D^-		H−		D^-	
LS(0)	20 860		20 864		20 788		20 796	
	20 833		20 837		20 765		20 775	
	20 804		20 808		20 739		20 750	
	20 767		20 772		20 703		20 711	
	20 751/49	2.8	20 755/53	2.6	20 692/87	4.8	20 700/696	4.8
	20 700.7		20 702.8		20 661.5		20 668.1	
	20 690.7		20 693.1		20 651.4		20 656.6	
LS(1)	20 906		20 910					
	20 879		20 883					
	20 842		20 847					
	20 808		20 811					
	20 784/83	1.7	20 787/86	1.7	20 693.3		20 696.2	
	20 726.6		20 728.8		20 685.1		20 688.3	
	20 717.9		20 720.3					
LS(2)	20 926				20 869		20 874	
	20 901/894	6.1	20 905/899	6.1	20 847/841	5.5	20 849/844	5.6
	20 856		20 861		20 811		20 813	
	20 823		20 827		20 780		20 784	
	20 801/798	3.3	20 804/802	2.2	20 759/756	2.7	20 764/762	2.8
	20 733.6		20 736.5		20 704.9		20 707.5	
	20 725.4		20 728.6		20 697.3		20 700.5	
LS(3)	20 776		20 782					
	20 746		20 751					
	20 706.9		20 712.5				20 688.6	
	20 701.8		20 706				20 674.9	
	20 612		20 612					
LS(4)	20 815		20 814					
	20 790/788	2.2	20 789/787	1.9				
	20 756		20 755					
	20 714		20 713					
	20 700/694	6.3	20 699/693	6.0				
	20 668.6		20 668.1					
	20 657.4		20 656.7					
LS(5)	20 913				20 860			
	20 867				20 824			
	20 836				20 794			
	20 813				20 773			
					20 693			
					20 690			

Figure 10(a) shows a polarized-bleaching sequence for the LS(1) center. Both laser polarizations produce bleaching. After the first cycle, there is a small recovery in the polarized fluorescence intensity on changing the excitation polarization by 90°. In comparison, the LS(2) center bleaches much more rapidly than the LS(1) center [Fig. 10(b)]. During the first cycle, both polarizations are bleached simultaneously. In subsequent cycles, the bleaching becomes polarization reversible. These bleaching sequences exhibited by the LS(1) and LS(2) centers resemble those reported for the Pr^{3+} $C_S(1)$ and $C_S(2)$ centers.[21]

The LS(3) and LS(4) centers exhibit bleaching behavior which is different from any observed for C_S centers of Pr^{3+}. Figure 10(c) shows that the bleaching sequence of the LS(3) center has the two polarizations bleaching semi-independently and without any recovery in the polarized

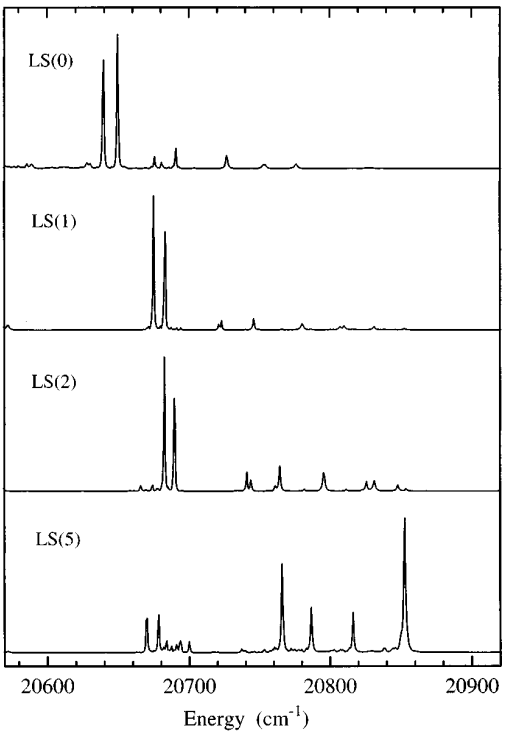

FIG. 7. 10-K selective excitation spectra of the $^5D_4$ multiplet for hydrogenated SrF_2:0.05%Tb^{3+}, while monitoring the LS(0) center fluorescence at 18 448 cm^{-1}, the LS(1) center at 18 425 cm^{-1}, the LS(2) center at 18 420 cm^{-1}, and the LS(5) center at 18 417 cm^{-1}.

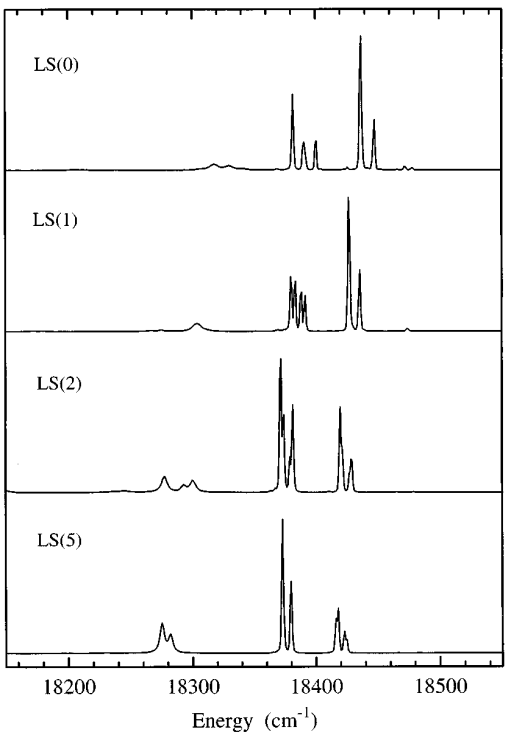

FIG. 8. 10-K $^5D_4 \rightarrow {}^7F_5$ fluorescence transitions of hydrogenated SrF_2:0.05%Tb^{3+}, for selective excitation of the LS(0) center at 20 651 cm^{-1}, the LS(1) center at 20 693 cm^{-1}, the LS(2) center at 20 705 cm^{-1}, and the LS(5) center at 20 860 cm^{-1}.

fluorescence on changing the excitation polarization. Unlike the bleaching of the LS(1) or LS(2) centers, nearly all of the fluorescence from the LS(3) center can be bleached to zero through long exposures to the excitation beam, as found for the Pr^{3+} $C_S(4)$ center.[21]

B. LS(4) center fluorescence enhancement

The bleaching curves obtained for the LS(4) center are remarkably unusual [Fig. 10(d)]. On pumping absorption transitions of the LS(4) center, the fluorescence intensity actually increases with exposure to the excitation beam. To our knowledge, this is the first time that such an enhancement in fluorescence has been observed upon selective excitation of a hydrogenic center. All the Pr^{3+}, Nd^{3+}, and Er^{3+} centers studied previously exhibited only fluorescence bleaching.[7,17,21] The increased intensity of the LS(4) center could always be removed by warming the crystal to above 100 K and recooling.

In a previously unradiated deuterated CaF_2:Tb^{3+} crystal, no fluorescence from the LS(4) center is observed when the shutter is first opened. Hence the LS(4) center is absent from a crystal which has been cooled from room temperature. In contrast, the hydrogenated CaF_2:Tb^{3+} crystal did show some LS(4) centers initially present.

It was observed visually that the path of green fluorescence caused by selectively exciting the LS(4) center increases in intensity with laser irradiation. If the excitation beam is moved, so that a new region of the crystal is exposed, almost all of the fluorescence is extinguished before

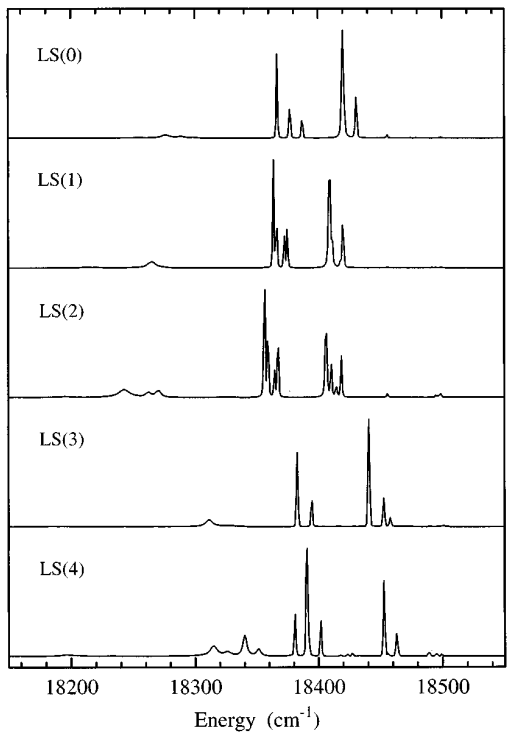

FIG. 9. 10-K $^5D_4 \rightarrow {}^7F_5$ fluorescence transitions of hydrogenated CaF_2:0.05%Tb^{3+}, for selective excitation of the LS(0) center at 20 691 cm^{-1}, the LS(1) center at 20 727 cm^{-1}, the LS(2) center at 20 734 cm^{-1}, the LS(3) center at 20 707 cm^{-1}, and the LS(4) center at 20 657 cm^{-1}.

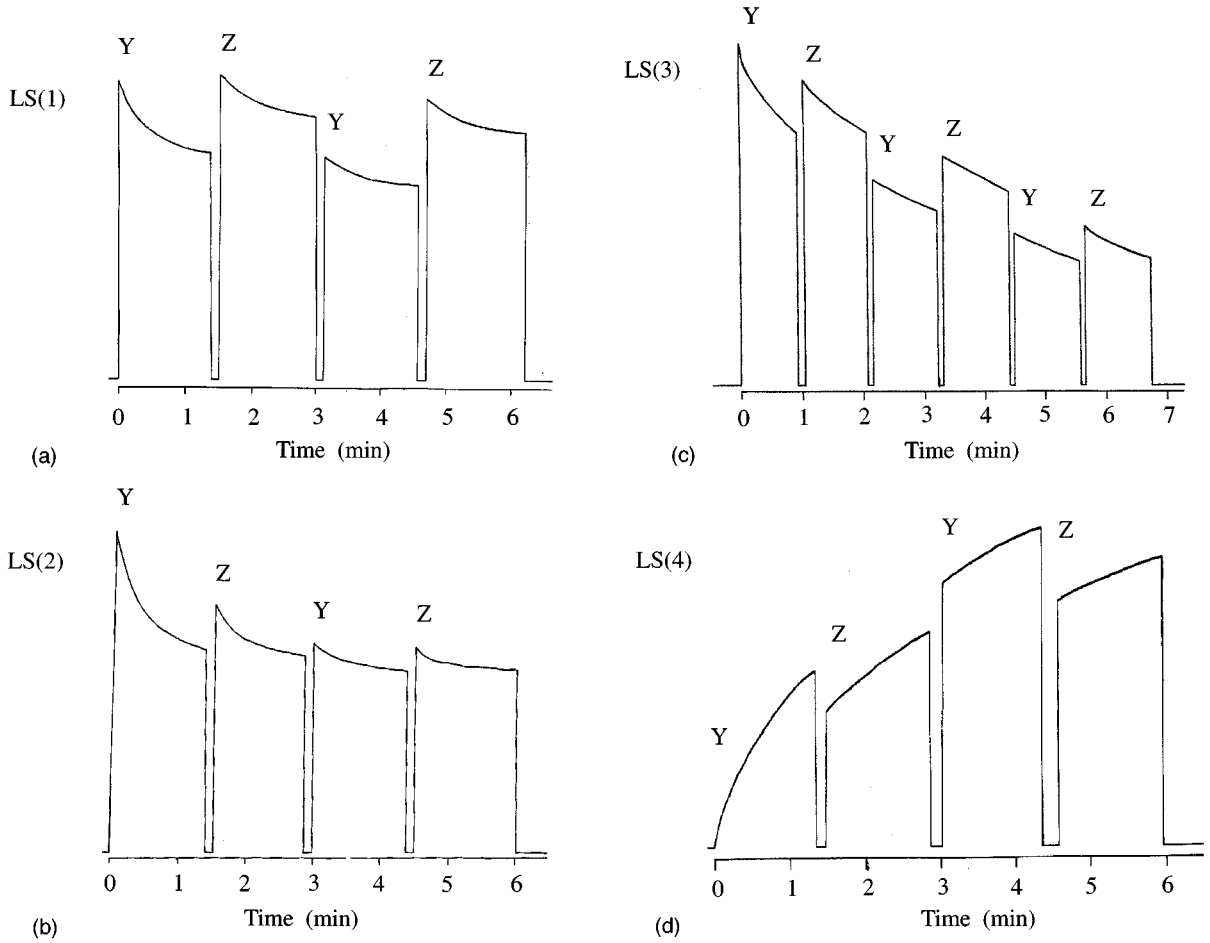

FIG. 10. Reversible polarized bleaching sequences of centers in the deuterated CaF_2:0.05%Tb^{3+} crystal, with an incident laser power of 15 mW. These were recorded during selective excitation of (a) the LS(1) center at 20 727 cm^{-1}, (b) the LS(2) center at 20 737 cm^{-1}, (c) the LS(3) center at 20 713 cm^{-1}, and (d) the LS(4) center at 20 668 cm^{-1}.

building up again. The intensity of the transmitted beam is not noticeably affected if the incident beam is quickly translated backwards and forwards through an exposed region of the crystal. This last result eliminates the possibility that the fluorescence enhancement is caused by saturated absorption of the excitation beam and subsequent bleaching.

It was found that the laser does not have to be resonant with any of the excitation transitions of the LS(4) center to achieve an enhancement in the fluorescence of this center. Indeed, the LS(4) center enhancement proceeded at a slower rate when pumping actual absorption transitions of the LS(4) center. Enhancement could even be achieved by tuning the laser to frequencies well below any excitation transitions of the LS(4) center. Quantitatively, 5 min of exposure to a 15-mW beam at 20 567 cm^{-1} increased the total fluorescence of the LS(4) center by a factor of 20, yet no particular excitation feature of the LS(4) center could be detected at this energy.

Broadband excitation spectra, obtained by monitoring fluorescence around 545 nm, were used to determine whether any other spectroscopic changes accompany this fluorescence enhancement. It was found that exposure to a weak 5-mW beam, for the few minutes required to produce an excitation spectrum, was enough to create a significant population of LS(4) centers. Subsequent excitation scans revealed further enhancement of the LS(4) center and bleaching of the LS(3) center fluorescence. The LS(1) and LS(2) centers remained unchanged over successive scans. This result suggest the LS(3) and LS(4) centers are related by a common bleaching mechanism.

It was found that the LS(3) center could also be bleached when the laser is detuned from any of its excitation transitions. As in the pervious example for the LS(4) center, the LS(3) center could be bleached when the laser is tuned to the arbitrary energy of 20 567 cm^{-1}. In that the population increase of the LS(4) center coincides with depopulation of the LS(3) center, the LS(4) center behaves like a photoproduct center of the LS(3) center.

C. Thermal reverting profiles of the LS(3) and LS(4) centers

Bleaching is a process in which the bleachable center crosses a potential barrier between two possible configurational states. If the LS(4) center is indeed a photoproduct of the LS(3) center, then the barrier potential associated with thermal restoration of the LS(3) center, through warming up the crystal, would be the same as that associated with thermal depletion of the LS(4) center. A thermal cycling sequence of warming the crystal up to successively higher set temperatures, holding it for 5 min, and then recooling, was used to obtain the thermal-restoration temperature profile of

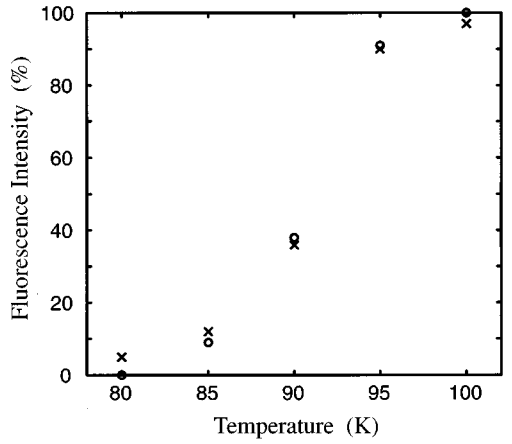

FIG. 11. Thermal depletion of the LS(4) center fluorescence intensity at 20 712 cm^{-1} (crosses) and thermal recovery of the LS(3) center fluorescence intensity at 20 657 cm^{-1} (circles). These values were obtained by thermal cycling of a deuterated CaF_2:0.05%Tb^{3+} crystal to different set temperatures.

the LS(3) center and the thermal-depletion temperature profile of the LS(4) center. Before each cycle the LS(3) center was rebleached to its original level. During this bleaching and for the subsequent fluorescence intensity measurements, the laser was tuned to the 20 712-cm^{-1} excitation line of the LS(3) center. Similarly, before each cycle to measure the thermal depletion of the LS(4) center, the LS(4) center population was prepared by tuning the laser to the 20 657-cm^{-1} excitation line of this center and irradiating the crystal.

Figure 11 shows that the thermal-restoration temperature profile of the LS(3) center was found to be identical to the thermal-depletion profile of the LS(4) center. This is strong evidence that the LS(4) center is indeed a photoproduct of the LS(3) center. The common reverting temperature is measured as (91±3) K, which corresponds to a potential barrier height[25] of around 2300 cm^{-1}, comparable to those determined for the C_S centers of Pr^{3+}. This thermal-reverting behavior discounts any possibility that the fluorescence enhancement of the LS(4) center is due solely to localized heating of the crystal caused by the laser beam itself.

The combined fluorescence bleaching and enhancement of the LS(3) and LS(4) centers is a process requiring absorption of the incident laser radiation by the Tb^{3+} centers. However, as the laser is not resonant with any of the electronic transitions of either center, the excitation mechanism is unclear.

The LS(3) center is unusual in being the only hydrogenic center found to have a photoproduct center with excitation transitions lower in energy than its own. The LS(3) center could be excited via phonon sidebands which have been observed extending down to 20 580 cm^{-1}. However, as these sidebands have only 1% of the intensity of the main electronic excitation lines, the LS(3) center would need to have a particularly high bleaching efficiency to account for its observed bleaching behavior. In any case, this phonon coupling hypothesis does not account for the nonresonant bleaching observed at 20 567 cm^{-1}, which is below the energy range of the phonon sidebands.

TABLE VI. Measured 10-K $^5D_4$ multiplet fluorescence lifetimes of Tb^{3+} centers in CaF_2:0.05%Tb^{3+} and SrF_2:0.05%Tb^{3+} crystals, in units of ms. The lifetimes for the hydrogenic centers have an uncertainty of ±0.2 ms.

Parent F^--centers	SrF_2		CaF_2	
C_{3v} F^-			5.9±0.3	
C_{4v} F^-	14.2±0.7		11.6±0.6	
Hydrogenic centers	H−	D^-	H−	D^-
LS(0)	3.90	4.30	3.65	3.96
LS(1)	3.77		3.71	4.19
LS(2)	3.62		3.40	3.56
LS(3)			3.37	3.62
LS(4)			3.92	
LS(5)	3.91			

The observation that the fluorescence enhancement of the LS(4) center occurs more slowly when the incident laser radiation is resonant with the LS(4) center excitation transitions suggests that the LS(4) center itself is also bleachable, but necessarily with an efficiency less than that of the LS(3) center. Such a difference between the relative bleaching efficiencies of these two centers would occur if the hydrogenic ions of the LS(4) center are less strongly coupled to the Tb^{3+} ion than are the hydrogenic ions of the LS(3) center. For each laser excitation energy and power there would be an equilibrium distribution of centers between the LS(3) and LS(4) configurations, which is determined by their relative bleaching rates. A test of this model arises from the expectation that a center in which the hydrogenic ions are more remote from the rare-earth ion should exhibit longer radiative lifetimes. This has been discussed for the $^1D_2$ multiplet fluorescence lifetimes of the different Pr^{3+} ion C_S centers.[22]

In the hydrogenated CaF_2:Tb^{3+} crystal both the LS(3) center and the LS(4) center are present when the crystal is cooled to 10 K from room temperature. This suggests that the double-well potential associated with these two hydrogen center configurations is nearly symmetric. This is still consistent with the proposed model in which their unusual bleaching behavior is ascribed to differences in their bleaching efficiencies, as distinct from differences in the respective barrier potentials which must be surmounted.

VI. FLUORESCENCE LIFETIMES

The 10-K $^5D_4$ multiplet lifetimes[11] of many Tb^{3+} centers were measured, and are given in Table VI. Not all the hydrogenic centers could be successfully discriminated by selective excitation using the 1.7-cm^{-1} linewidth of the pulsed N_2 laser system, which prevented their fluorescence lifetime measurement. The Tb^{3+} centers have an energy gap of 14 000 cm^{-1} to the next lower $^7F_0$ multiplet, which is large enough to preclude any significant nonradiative decay through the CaF_2 or SrF_2 lattice phonons or through hydrogenic ion local mode vibrations. Hence radiative decay is the dominant process.

The CaF_2 C_{4v} F^-, LS(0) H^-, and LS(0) D^- center lifetimes are all remarkably similar to those of the $^6P_{7/2}$ multiplet of the Gd^{3+} C_{4v} F^-, H^-, and D^- centers in CaF_2, whose 77-K values are 11 ms for the F^- center, 4 ms for the H^-

center, and 3.5 ms for the D^- center.[26] This confirms that radiative decay is the dominant relaxation process for the Tb^{3+} centers.

The similar Gd^{3+} and Tb^{3+} lifetimes for a given C_{4v} center arise from summation over all possible electric-dipole radiative pathways to lower crystal-field levels. Closure then yields a limiting common value for given crystal-field parameter values.

A. Parent F^--charge-compensated Tb^{3+} centers

As for CaF_2:Er^{3+}[7] and CaF_2:Ho^{3+},[10] the Tb^{3+} trigonal *B* center has a generally shorter lifetime than the C_{4v} center, reflecting the different crystal fields experienced by the rare-earth ions in each respective center. The shorter fluorescence lifetime of the trigonal centers suggests a charge-compensation modification of the eight nearest-neighbor F^- ions around the R^{3+} ion, rather than just a single F^- ion in the next-nearest-neighbor position located along a $\langle 111 \rangle$ direction from the R^{3+} ion.

As for other rare-earth centers, the CaF_2 center lifetimes are shorter than the SrF_2 center lifetimes, a consequence of the magnitudes of their respective crystal-fields. For electric-dipole-allowed radiative transitions, the transition probabilities and hence radiative relaxation rates vary as the square of matrix elements of the odd-parity terms of the crystal field.[27] With the expectation that the odd and even terms of the crystal field scale by similar ratios in going between centers of identical ion geometry, the transition probabilities would be expected to vary as the squares of the respective even-term crystal-field parameters. For the Tb^{3+} ion C_{4v} F^- centers the ratio of the $^5D_4$ multiplet lifetimes for SrF_2 relative to CaF_2 is 1.22 ± 0.12. From the crystal-field parameters of Table IV, a scalar crystal-field strength parameter[28] can be derived with values of 890 and 690 cm^{-1} for CaF_2 and SrF_2 , respectively. The ratio of the squares of these values is 1.65.

For comparison, the Nd^{3+} C_{4v} F^- centers in CaF_2 and SrF_2 have a lifetime ratio of 1.13 ± 0.07 for the $^4F_{3/2}$ multiplet, while the square of the crystal-field strength parameters is 1.30. For the Ho^{3+} C_{4v} F^- centers the lifetime ratio for the $^5S_2$ multiplet is 1.40 ± 0.06, which matches the 1.38 ratio of the corresponding crystal-field strength parameters for the Ho^{3+} C_{4v} centers. The larger discrepancy found for Tb^{3+} may be the result of significant magnetic-dipole contributions to the radiative relaxation from the $^5D_4$ multiplet. For C_{4v} centers, such contributions would be essentially independent of the respective crystal-field strengths.

B. Hydrogenic Tb^{3+} centers

The lifetimes of the hydrogenic C_{4v} centers are shorter than those of the C_{4v} F^- centers by a factor of 3.6 for SrF_2 and 3.2 for CaF_2 (Table VI). These lifetime trends are accounted for by 1.8 times larger crystal fields for the hydrogenic C_{4v} centers, as was found for the purely radiative lifetimes of the Gd^{3+} C_{4v} centers.[26]

The H^- lifetimes are at most 10% shorter than those of the D^- centers for both CaF_2 and SrF_2 (Table VI). The near-equality of these H^- and D^- lifetimes for a given center confirms their radiative nature.

In contrast, the Pr^{3+} $^3P_0$ and $^1D_2$ multiplet and Nd^{3+} $^4F_{3/2}$ multiplet lifetimes for the hydrogenic C_{4v} centers are dominated by nonradiative decay processes involving the respective local-mode phonons. The involvement of such phonons in the decay is shown by the greatly reduced H^- center lifetimes compared to those for the D^- centers.[29]

All the LS center fluorescence lifetimes are comparable, consistent with essentially radiative lifetimes for fluorescence transitions of all these centers from the $^5D_4$ multiplet. As their lifetime values center around that of the hydrogenic LS(0) center and not that of the C_{4v} F^- center, all the LS centers necessarily have interstitial hydrogenic ion charge compensation.

VII. CONCLUSION

Sets of energy levels established for the C_{4v} F^- centers of Tb^{3+} in CaF_2 and SrF_2 provide the basis for crystal-field fits and polarization analyses, which require consideration of magnetic-dipole contributions to the observed transitions. Both the quality of the crystal-field fit to the experimental energy levels and the successful interpretation of the measured polarization ratios confirm the Tb^{3+} C_{4v} site symmetry assignment for these C_{4v} F^- centers.

The hydrogenic C_{4v} and related bleachable centers form sets of centers bearing similarities to those observed for Pr^{3+}, Nd^{3+}, and Er^{3+}. Results of a study of bleaching centers in hydrogenated and deuterated CaF_2:Tb^{3+} and SrF_2:Tb^{3+} revealed the unusual phenomenon of enhanced fluorescence under laser excitation for the LS(4) center, which is related to the LS(3) center as a photoproduct. Further studies are needed to understand this bleaching behavior. The $^5D_4$ multiplet fluorescence lifetimes for all the Tb^{3+} centers measured are essentially radiative, being similar for H^- and D^- varieties of the same center, as was the case for hydrogenic Gd^{3+} centers.

ACKNOWLEDGMENTS

This research was supported by the University of Canterbury and the New Zealand Lottery Board through Research Grants. We wish to thank Jon Paul Wells for Zeeman infrared spectra and Michael F. Reid for providing his crystal-field fitting program. We also wish to thank Ron Culley, Ross Ritchie, Clive Rowe, and Wayne Smith for technical assistance.

*Corresponding author. Present address: Inorganic Chemistry Laboratory, University of Oxford, South Parks Rd., Oxford OX1 3QR, England.

[1] N. Rabbiner, J. Opt. Soc. Am. **55**, 436 (1965).

[2] N. Rabbiner, J. Opt. Soc. Am. **57**, 217 (1967).

[3] D. Narayana Rao, P. Venkateswarlu, and D. Ramachandra Rao, Indian J. Phys. **54B**, 305 (1980).

[4] J. Chrysochoos, J. Less-Common Met. **93**, 73 (1983).

[5] P. A. Forrester and C. F. Hempstead, Phys. Rev. **126**, 923 (1963).

[6] A. A. Antipin, L. D. Livanova, and L. Y. Shekun, Fiz. Tverd.

Tela (Leningrad) **10**, 1286 (1968) [Sov. Phys. Solid State **10**, 1025 (1968)].
[7] N. J. Cockroft, D. Thompson, G. D. Jones, and R. W. G. Syme, J. Chem. Phys. **86**, 521 (1987).
[8] N. J. Cockroft, G. D. Jones, and R. W. G. Syme, J. Chem. Phys. **92**, 2166 (1990).
[9] H. K. Welsh, J. Phys. C **18**, 5637 (1985).
[10] M. Mujaji, G. D. Jones, and R. W. G. Syme, Phys. Rev. B **46**, 14 398 (1992).
[11] G. D. Jones and K. M. Murdoch, J. Lumin. **60&61**, 131 (1994).
[12] R. J. Elliott, W. Hayes, G. D. Jones, H. F. Macdonald, and C. T. Sennett, Proc. R. Soc. London Ser. A **289**, 1 (1965).
[13] R. J. Reeves, G. D. Jones, and R. W. G. Syme, Phys. Rev. B **46**, 5939 (1992).
[14] Y. L. Khong, G. D. Jones, and R. W. G. Syme, Phys. Rev. B **48**, 672 (1993).
[15] R. W. Schwartz, H. G. Brittain, J. P. Riehl, W. Yeakel, and F. S. Richardson, Mol. Phys. **34**, 361 (1977).
[16] F. S. Richardson and T. R. Faulkner, J. Chem. Phys. **76**, 1595 (1982); J. D. Saxe, J. P. Morley, and F. S. Richardson, Mol. Phys. **47**, 407 (1982).
[17] T. P. J. Han, G. D. Jones, and R. W. G. Syme, Phys. Rev. B **47**, 14 706 (1993).
[18] W. T. Carnall, G. L. Goodman, K. Rajnak, and R. S. Rana, J. Chem. Phys. **90**, 3443 (1989).
[19] K. R. Lea, M. J. M. Leask, and W. P. Wolf, J. Phys. Chem. Solids **23**, 1381 (1962).
[20] M. F. Reid, J. J. Dallara, and F. S. Richardson, J. Chem. Phys. **79**, 5743 (1983).
[21] R. J. Reeves, G. D. Jones, and R. W. G. Syme, Phys. Rev. B **40**, 6475 (1989).
[22] K. M. Murdoch, Ph.D. thesis, University of Canterbury, Christchurch, New Zealand, 1993.
[23] A. Edgar, G. D. Jones, and M. R. Presland, J. Phys. C **12**, 1569 (1979).
[24] N. J. Cockroft, T. P. J. Han, R. J. Reeves, G. D. Jones, and R. W. G. Syme, Opt. Lett. **12**, 36 (1987).
[25] U. Bogner (private communication).
[26] G. D. Jones, S. Peled, S. Rosenwaks, and S. Yatsiv, Phys. Rev. **183**, 353 (1969).
[27] B. G. Wybourne, *Spectroscopic Properties of Rare Earths* (Interscience, New York, 1965).
[28] F. Auzel and O. L. Multa, J. Phys. **44**, 201 (1983).
[29] R. J. Reeves, G. D. Jones, N. J. Cockroft, T. P. J. Han, and R. W. G. Syme, J. Lumin. **38**, 198 (1987).